

Defect-induced supersolidity with soft-core Bosons

F. Cinti,¹ T. Macrì,¹ W. Lechner,² G. Pupillo,³ and T. Pohl¹

¹Max Planck Institute for the Physics of Complex Systems, Nöthnitzer Str. 38, 01187 Dresden, Germany

²IQOQI and Institute for Theoretical Physics, University of Innsbruck, Austria

³IPCMS (UMR 7504) and ISIS (UMR 7006), Université de Strasbourg and CNRS, Strasbourg, France

We determine the zero-temperature phase diagram of two-dimensional Bosons with finite-range soft-core interactions. For high particle densities, we demonstrate that the ground state can be a commensurate density-wave-type supersolid. For low densities, the system is shown to form a solid in which superfluidity is provided by delocalized zero-point defects. This provides the first example of continuous-space supersolidity consistent with the Andreev-Lifshitz-Chester scenario.

PACS numbers: 67.80.K-, 05.30.Jp, 02.70.Ss

Spontaneous symmetry breaking is a focal principle of condensed matter physics – yet, simultaneous breaking of fundamentally different symmetries represents a rare and exotic phenomenon. A prime example is the so-called supersolid state [1], which displays both crystalline and superfluid properties, i.e. the simultaneous breaking of continuous translational and global gauge symmetry. The first mentioning of such a state goes back to Gross [2], who discovered a density-modulated superfluid emerging from a simple mean-field model for solid Helium. While this picture turned out too simplistic for real crystals, it was later shown [3, 4] that supersolidity can still exist under two key assumptions: (i) that the ground state of a bosonic crystal contains defects such as vacancies and interstitials, and (ii) that these defects are delocalized, thereby, giving rise to superfluidity. Forty years after its conjecture by Andreev and Lifshitz [3] and Chester [4] (ALC) the precise physical nature and mere existence of this enigmatic phase of matter has since remained under active debate [5].

In 2004 Kim and Chan provided first suggestive evidence for superfluidity in solid ^4He in torsional oscillator experiments [6]. Their discovery has sparked a host of new experimental activity [7] that qualitatively confirmed this first observation, but also led to contrasting interpretations. Theoretical work has established that crystal incommensurability is a necessary condition for superfluidity [8] and that zero-point defects in ground state solid He are prevented by a large activation energy [9, 10]. In addition, Refs. [10–13] have shown that point-like defects experience an effective attraction that results in defect-clustering and phase separation, ruling out the possibility of defect-induced supersolidity [10] as in the ALC scenario. Very recent experiments have finally shown that the original observations [6] were caused by shear modulus stiffening of bulk solid He, and found no signature of superfluidity upon avoiding this undesired effect [14]. As a result, there now seems to be consistent experimental and theoretical evidence for the absence of the long-sought supersolid phase in He. The mere existence of free-space *supersolidity in any type of quantum*

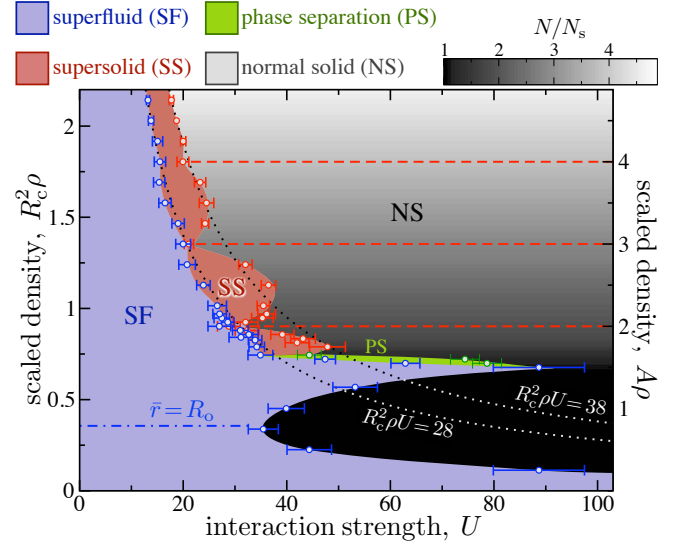


FIG. 1: (color online) Zero temperature-limit phase diagram of two-dimensional soft-core Bosons described by eq.(1) displaying the emergence of superfluid (SF) and different solid (NS) and supersolid (SS) phases for varying interaction strength U and density ρ . For the left y -axis the density has been scaled by the soft-core radius R_c , while the right axis gives the density in units of the inverse area, $A = \sqrt{3}(1.6R_c)^2/2$, of the unit cell of the high-density solid phase, corresponding to the lattice site occupation N/N_s for a given number of particles and lattice sites, N and N_s , respectively. The grey region labeled as NS for $A \gtrsim 1.5$ corresponds to a cluster crystal. Supersolid phases with different occupation numbers are found between two hyperbolas, defined by $R_c^2 \rho U = \text{const}$ (dotted lines). At high densities ($A \rho \gtrsim 3.5$) they can be understood in terms of density modulated superfluids, while superfluidity within the low-density supersolid lobes emerges from delocalized zero-point defects.

solid thus remains an open question.

In this Letter, we show that a quantum gas of bosonic particles interacting via soft-core potentials provides a prototype system that realizes all of the described phases. Using exact numerical techniques, we determine the complete zero-temperature phase diagram which, in addi-

tion to a superfluid and normal crystal phase, contains a density-wave supersolidity. Most importantly, this system is shown to form incommensurate superfluid ground-state solids – providing the first example of defect-induced supersolidity as conjectured by ALC [3, 4].

We consider a two-dimensional ensemble of N Bosons with density ρ , interacting via a pair potential of the type $V(r) = V_0/(r^\gamma + R_c^\gamma)$. This interaction approaches a constant value V_0 as the inter-particle distance, r , decreases below a critical soft-core distance R_c , and drops to zero for $r > R_c$. The limiting case $\gamma \rightarrow \infty$ yields the soft-disc model [15], while $\gamma = 3$ and $\gamma = 6$ correspond to soft-core dipole-dipole [16, 17] and van der Waals [18] interactions that can be realized with ultracold atoms [18, 19] or polar molecules [20, 21]. Here, we focus on the latter case ($\gamma = 6$), for which the Hamiltonian reads

$$\hat{H} = - \sum_{i=1}^N \frac{\nabla_i^2}{2} + \sum_{i < j}^N \frac{U}{1 + r_{ij}^6}. \quad (1)$$

where the units of length and energy are R_c and \hbar^2/mR_c^2 , respectively, and m denotes the particle mass. In these units, the system behavior is controlled by the dimensionless interaction strength $U = mV_0/(\hbar^2 R_c^4)$ and the dimensionless density $R_c^2 \rho$.

Particles with soft-core interactions have been studied previously in the field of soft condensed matter physics [22, 23], in the classical high-temperature regime. One of the main findings has been that pair potentials with a negative Fourier component [22] favor the formation of particle clusters, which in turn can crystallize to form a so-called cluster-crystal. In the quantum regime, theoretical work has so far focused on the regime of weak interactions and high particle densities [16, 18, 24–27], which was shown to be well described by mean-field calculations [28, 29]. In this limit, one finds strongly modulated superfluid states [15, 16, 18], corresponding to a density-wave supersolid as originally conjectured by Gross [2].

Here, we investigate the so far unexplored domain of large interaction strengths and low particle densities, where strong correlations and quantum fluctuations are expected to become important. We employ path integral Monte Carlo (PIMC) simulations [30] based on the continuous space worm algorithm [31] to determine the equilibrium properties of the Hamiltonian (1) in the canonical ensemble, i.e. at fixed density and temperature. An accurate determination of the ground state in the thermodynamic limit is obtained by decreasing the temperature to very small values sufficiently below \hbar^2/mR_c^2 and by increasing the system size until we reach convergence of relevant physical observables, such as the superfluid fraction f_s and density-density correlation functions $g_2(r)$, see e.g. [1, 16]. These quantities are used to distinguish, e.g., between the superfluid phase (finite value of f_s), the crystalline phase (large density modulations in $g_2(r)$ and

vanishing f_s) and supersolid phase (large density modulations in $g_2(r)$ and finite f_s).

The obtained phase diagram, shown in Fig.1, reveals a rich spectrum of phases with varying interaction strength and density. At small densities $R_c^2 \rho \lesssim 0.5$ we find two phases: a superfluid and an insulating triangular crystal composed of $N_s = N$ singly occupied sites, being N_s and N the number of sites and the total number of particles, respectively. The observed lobe structure of this crystalline region is readily understood by noticing that at very low densities, i.e. large inter-particle distances $\bar{r} = 1/\sqrt{\pi\rho} > R_c$, the physics is dominated by the long-range tail of the interaction potential, $V \sim 1/r^6$. For a fixed interaction strength $U \gtrsim 35$, we thus find a first order liquid-solid quantum phase transition with increasing $A\rho$, consistent with previous work on Bosons with power-law interactions [20, 32–34]. However, in marked contrast to such systems, here the repulsion weakens as the particle distance approaches the soft-core radius R_c and declines dramatically beyond the turning point $R_o = (5/7)^{1/6} R_c$. Consequently, the crystal melts again for increasing density ($\bar{r} < R_o$) leading to a reentrant superfluid. Indeed, the resulting insulating lobe is centered around the density at which $\bar{r} = R_o$, as indicated in Fig.1.

A distinctive consequence of the soft-core interaction is that the energy cost for forming close particle pairs is bound by V_0 . This potentially enables the formation of crystalline phases with $N > N_s$ above a critical density where doubly occupied lattice sites become energetically favorable upon increasing the lattice constant. As expected for a triangular crystal, the lattice constant decreases as $a = (\sqrt{3}\rho/2)^{-1/2}$ at small densities. However, around $a \approx 1.4 R_c$ it increases again and settles to a density-independent value of $a_0 \simeq 1.6 R_c$ upon further increase of ρ . The corresponding volume of the unit cell $A = \sqrt{3}/4 a_0^2$ provides a measure of the lattice occupancy $N/N_s = A\rho$, which is shown in Fig.1. The transition to cluster crystals occurs at $A\rho \approx 1.5$, which indeed coincides with the critical density for crystallization of the reentrant superfluid phase.

Around this density, a thin region of phase separation is found to lay in between the cluster crystal and the superfluid phase. Fig.2(b) shows a typical example for the particles density in this region. Two distinct coexisting phases can be recognized: a crystal phase with exactly two particles per site (upper part of the figure), and a superfluid phase (lower part). We have carefully checked that the occurrence of this phase-separated state is not an artifact of the simulations, by performing accurate annealing and by choosing different initial conditions, such as random and different crystalline configurations.

Above incommensurate lattice occupations $N/N_s \gtrsim 1.5$, the direct liquid-solid quantum phase transition is replaced by a first order transition from a superfluid to a supersolid phase. The SS phase is approximately

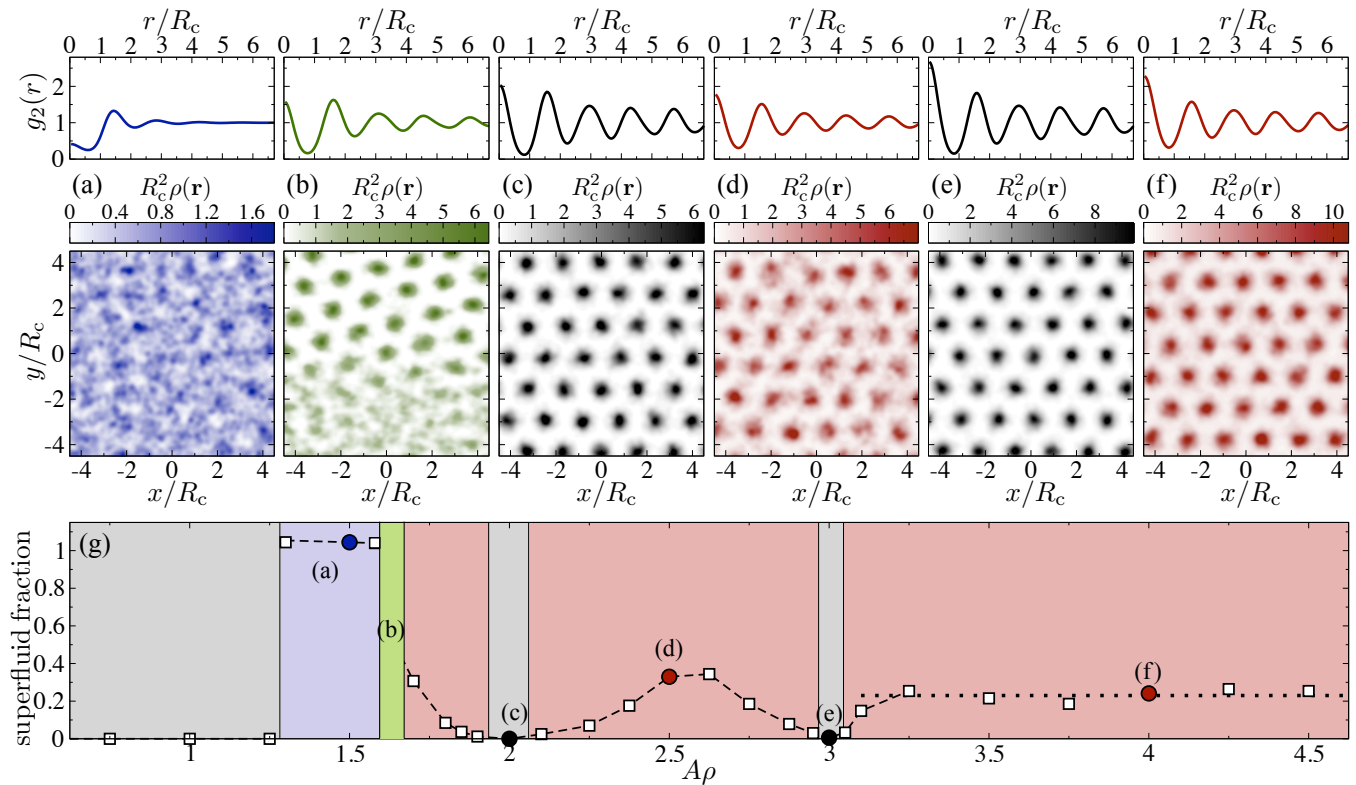


FIG. 2: (color online) (a)-(f) Two-point correlation function $g_2(r)$ (angle-averaged) and density distribution $\rho(\mathbf{r})$ for $\rho R_0^2 U = 32$ and different values of $A\rho$, indicated in panel (g), showing the superfluid fraction f_s as a function of $A\rho$ across the different phases of Fig.1. The horizontal dotted line shows the $\rho \rightarrow \infty$ limit of f_s for a density-wave supersolid, obtained from a mean field evaluation according to Ref. [35].

found to occur between the two hyperbola defined by $R_c^2 \rho U = \alpha$, with $\alpha \approx 28$ and $\alpha \approx 38$, respectively (see dotted lines in Fig.1). These two lines are derived from the weak interaction limit ($U \rightarrow 0$ and $\rho \rightarrow \infty$ with $\alpha = \text{const.}$), where mean-field theory predicts a transition to a density-wave supersolid that is determined only by the value of α [18]. While mean-field predictions are essentially exact for densities $A\rho \gtrsim 4$ (see Fig.1), the situation is dramatically different at smaller densities where the discrete nature of the particles plays a significant role. This gives rise to the emergence of supersolid regions with a lobe structure, which vanish at commensurate lattice occupations $N/N_s = 2$ and $N/N_s = 3$. There, we find a direct transition between a superfluid and an insulating solid phase.

This behavior is illustrated in Fig.2, where the superfluid fraction, f_s , is shown as a function of $A\rho$ for $\alpha = 32$, i.e. in between the two dotted lines in Fig.1. As shown in Fig.2(c) and (e), at $A\rho = 2$ and $A\rho = 3$ one finds a commensurate crystal with exactly $N/N_s = 2$ [Fig.2(c)] and $N/N_s = 3$ [Fig.2(e)] per lattice site, respectively, and vanishing superfluidity [Fig.2(g)]. Importantly, the crystal structure in between these two densities is practically unchanged, as seen by comparing the particle density and

density-density correlation function $g_2(r)$ (averaged over angles) in Figs.2(c)-(e). However, the incommensurate lattice filling N/N_s and the resulting fluctuations of individual occupations enables particles to tunnel between the sites. This gives rise to a non-vanishing superfluid fraction of the crystal, which can assume sizable values of $f_s = 0.3$ for $N/N_s \approx A\rho = 2.5$.

For higher densities $A\rho > 3$, the scenario described above changes considerably. As shown in Fig.2(g) the superfluid fraction approaches a constant, density-independent value $f_s \approx 0.24$ with increasing ρ . In particular, for an average commensurate filling $N/N_s = 4$ there is no direct phase transition between a superfluid and a solid insulating phase, and instead the supersolid phase persists with no significant difference to the case of incommensurate lattice occupancies $N/N_s \neq 4$. This behavior signals a crossover to the regime where the supersolid phase can be understood in terms of a density modulated superfluid [2, 15, 16, 18, 28], where the discrete nature of the particles becomes irrelevant. In this limit, the superfluid-supersolid quantum phase transition is well captured within a mean-field description [15, 18, 29], which predicts a transition point at $\alpha = R_c^2 \rho U = 28.2$ as well as a superfluid fraction $f_s = 0.23$ that is solely

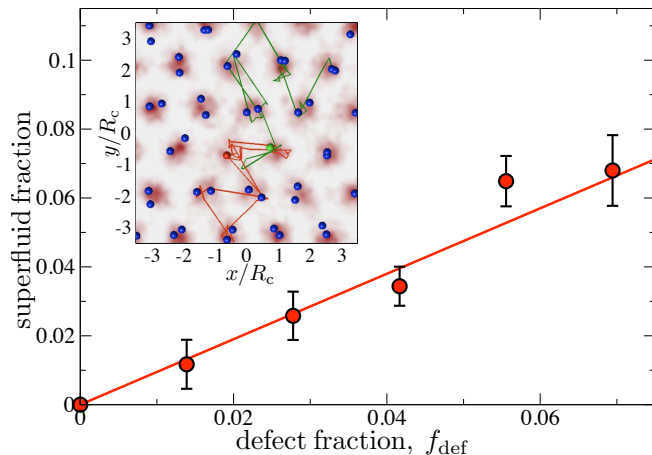


FIG. 3: (color online) Superfluid fraction in a doubly occupied solid ($N/N_s = 2$) as a function of the fraction of defects in the form of singly occupied sites. Here we fixed $U = 31$, $N_s = 72$, and $N = 139 \div 144$. The inset shows the particle density (color code) for $f_{\text{def}} = 0.03$, obtained from a PIMC configuration along with the particle positions for a single imaginary-time slice. There are two singly occupied sites, which are highly mobile as indicated by the corresponding imaginary-time trajectories.

determined by α . As shown in Figs.1 and 2(g) this is well confirmed by our PIMC results for $A\rho \gtrsim 3.5$, suggesting that the transition to density-wave supersolidity takes place at a small particle number per lattice site.

The most interesting behavior takes place around the superfluid-solid quantum phase transition at $N/N_s = 2$. Figure 3 provides a more detailed look at the transition between the insulating crystal and the supersolid phase close to $R_c^2 \rho U \approx 28$ ($U = 31$). Starting from the insulating solid with doubly occupied lattice sites, we successively remove a small number of particles from randomly chosen sites and monitor the superfluid fraction of the resulting new groundstate obtained from our PIMC simulations. Removing a small number of particles does not cause structural changes of the ground state but rather creates a small fraction $f_{\text{def}} = (2N_s - N)/N_s$ of zero-point crystal defects in the form of singly occupied sites. An analysis of our PIMC configurations shows that defects do not cluster and instead delocalise, as illustrated in the inset of Fig.3. Indeed, we find a finite superfluid fraction even for small defect concentrations, which increases linearly with f_{def} . We have checked that this behaviour is pertinent to the groundstate and not to a metastable configuration by running simulations with different initial conditions, including clustered defects. This behaviour is thus consistent with defect-induced supersolidity according to the ALC scenario, and constitutes the central result of this work.

Supersolidity in this system is the consequence of two unique features of soft bosons. (i) The energy cost for

forming close particle pairs is bound by V_0 , which facilitates the formation of cluster crystals that naturally entail zero-point defects. (ii) The dynamics and interaction of these defects differs fundamentally from those of conventional solids. In the latter case, vacancies and interstitials induce displacement fields that lead to purely attractive defect-interactions [10, 12, 13, 36] and, thereby, prevent a delocalization of defects [10]. In cluster solids, on the other hand, defect interactions are purely repulsive, since two interstitials interact via essentially the same underlying particle interaction $V(r)$ of eq. (1). The same applies to vacancies due to particle-hole symmetry around integer N/N_s . In the present case, the transition between these two regimes is controlled by the particle density. For $A\rho \gtrsim 1.5$ delocalized zero-point defects allow for the formation of supersolid phases. Below this density particles do not explore the soft core part of the interaction potential, such that defects are attractive and supersolidity is absent consistent with the results of Ref. [10]. Around the transition region $A\rho \approx 1.5$ neither picture applies, and one observes separation between a superfluid and a doubly occupied, insulating cluster solid. Preliminary calculations based on path integral Langevin dynamics [37] suggest that in this region structural and dynamical heterogeneity gives rise to a quantum glass phase at finite temperature.

Having identified a physical system that facilitates defect-induced supersolidity, we hope that this work will provide useful guidance for future experiments and initiate further theoretical explorations. An important question concerns the general features of the interaction potential that are required to maintain the type of supersolid states described in this work. While the emergence of density-wave supersolids is largely insensitive to the detailed shape of the soft-core interaction, the low-density physics described in this work may be strongly affected. In fact, it seems reasonable to expect an interesting competition between intra- and inter-site interactions within the self-assembled crystal that will strongly depend on the long-range tail of the particle interactions. While we have focussed here on two-dimensional systems, the role of the dimensionality represents another outstanding issue, and in particular its role for frustration effects that may be decisive for defect delocalization. While the considered interactions do not straightforwardly occur in natural crystals, we note that so-called Rydberg dressing [18, 19, 38–40] of atomic Bose-Einstein condensates constitutes a promising approach for an experimental realization. Ultimately, the characterization of a broad class of suitable interactions and conditions will greatly ease the search for viable implementations. At this point, ultracold atoms and molecules appear most promising, as they offer a great deal of flexibility in designing various types of long-range interactions [20, 21].

We thank M. Boninsegni, S. Pilati, N. V. Prokof'ev, and S. G. Söyler for fruitful and valuable discussions. This work was supported by the EU through the ITN COHERENCE. G P is supported by the ERC-St Grant "ColDSIM" (grant agreement 307688) and EOARD.

-
- [1] M. Boninsegni and N. V. Prokofev, *Rev. Mod. Phys.* **84**, 759 (2012).
 - [2] E. P. Gross., *Phys. Rev.* **106**, 161 (1957).
 - [3] A. F. Andreev and I. M. Lifshitz, *JETP* **29**, 1107 (1969).
 - [4] G. V. Chester, *Phys. Rev. A* **2**, 256 (1970).
 - [5] S. Balibar, *Nature* **464**, 176 (2010).
 - [6] E. Kim and M. H. W. Chan, *Nature* **427**, 225 (2004); *Science* **305** 1941, (2004).
 - [7] A. S. Rittner and J. Reppy, *Phys. Rev. Lett.* **97**, 165301 (2006); *Phys. Rev. Lett.* **98**, 175302 (2007); M. Kondo et al., *J. Low Temp. Phys.* **148** 695 (2007); Y. Aoki, J. C. Graves and H. Kojima, *Phys. Rev. Lett.* **99**, 015301 (2007); J. Day and J. Beamish, *Nature* **450**, 853 (2007); Hunt, B. et al., *Science* **324**, 632 (2009); J. T. West, X. Lin, Z. G. Cheng and M. H. Chan, *Phys. Rev. Lett.* **102**, 185302 (2009); J. D. Reppy, *Phys. Rev. Lett.* **104**, 255301 (2010); H. Choi et al., *Phys. Rev. Lett.* **108**, 105302 (2012); X. Mi and J. D. Reppy, *Phys. Rev. Lett.* **108**, 225305 (2012).
 - [8] N. Prokofev and B. Svistunov, *Phys. Rev. Lett.* **94**, 155302 (2005).
 - [9] D. M. Ceperley and B. Bernu, *Phys. Rev. Lett.* **93**, 155303 (2004).
 - [10] M. Boninsegni et al., *Phys. Rev. Lett.* **97**, 080401 (2006).
 - [11] R. Rota and J. Boronat, *Phys. Rev. Lett.* **108**, 045308 (2012).
 - [12] P.N. Ma, L. Pollet, M. Troyer and F.-C. Zhang, *J. of Low Temp. Phys.*, **152**, 156 (2008).
 - [13] W. Lechner and C. Dellago, *Soft Matter* **5**, 646 (2009).
 - [14] D. Y. Kim and M. H. W. Chan, *Phys. Rev. Lett.* **109**, 155301 (2012).
 - [15] Y. Pomeau and S. Rica, *Phys. Rev. Lett.* **72**, 2426 (1994).
 - [16] F. Cinti, P. Jain, M. Boninsegni, A. Micheli, P. Zoller, and G. Pupillo, *Phys. Rev. Lett.* **105**, 135301 (2010).
 - [17] X. Li, W. V. Liu, and C. Lin, *Phys. Rev. A* **83**, 021602 (2011).
 - [18] N. Henkel, R. Nath, and T. Pohl, *Phys. Rev. Lett.* **104**, 195302 (2010).
 - [19] F. Maucher et al., *Phys. Rev. Lett.* **106** 170401, (2011).
 - [20] H. P. Büchler et al., *Phys. Rev. Lett.* **98**, 060404 (2007).
 - [21] A. Micheli, G. Pupillo, H. P. Büchler and P. Zoller, *Phys. Rev. A* **76**, 043604 (2007).
 - [22] C. N. Likos, A. Lang, M. Watzlawek, and H. Löwen, *Phys. Rev. E* **63**, 031206 (2001).
 - [23] B. M. Mladek et al., *Phys. Rev. Lett.* **96**, 045701 (2006); C. N. Likos, B. M. Mladek, D. Gottwald, and G. Kahl *J. Chem. Phys.* **126**, 224502 (2007); B M. Mladek, P. Charbonneau, and D. Frenkel, *Phys. Rev. Lett.* **99**, 235702 (2007); D. Coslovich, L. Strauss and G. Kahl, *Soft Matter* **7**, 2127 (2011).
 - [24] N. Sepulveda, C. Josserand, and S. Rica, *Eur. Phys. J. B* **78**, 439 (2010).
 - [25] S. Saccani, S. Moroni, and M. Boninsegni, *Phys. Rev. B* **83**, 092506 (2011).
 - [26] M. Kunimi and Y. Kato, *Phys. Rev. B* **86**, 060510 (2012).
 - [27] P. Mason, C. Josserand and S. Rica, *Phys. Rev. Lett.* **109**, 045301 (2012).
 - [28] N. Henkel, F. Cinti, P. Jain, G. Pupillo, and T. Pohl, *Phys. Rev. Lett.* **108**, 265301 (2012).
 - [29] T. Macrì, F. Maucher, F. Cinti, and T. Pohl, *arXiv:1212.6934v1* (2012).
 - [30] D. M. Ceperley., *Rev. Mod. Phys.* **67**, 279 (1995).
 - [31] M. Boninsegni, N. Prokofev, and B. Svistunov, *Phys. Rev. Lett.* **96**, 070601 (2006).
 - [32] G. E. Astrakharchik, J. Boronat, I. L. Kurbakov, and Y. E. Lozovik, *Phys. Rev. Lett.* **98**, 060405 2007.
 - [33] C. Mora, O. Parcollet, and X. Waintal, *Phys. Rev. B* **76**, 064511 (2007).
 - [34] O. N. Osychenko et al., *Phys. Rev. A* **84**, 063621 (2011).
 - [35] A. J. Leggett, *Phys. Rev. Lett.* **25**, 1543 (1970).
 - [36] W. Lechner and C. Dellago, *Soft Matter* **5**, 2752 (2009).
 - [37] M. Ceriotti, M. Parrinello, T. E. Markland, and D. E. Manolopoulos, *J. Chem. Phys.* **133**, 124104 (2010); T. E. Markland, J. A. Morrone, K. Miyazaki, B. J. Berne, D. R. Reichman, and E. Rabani, *J. Chem. Phys.* **136**, 074511 (2012).
 - [38] L. Santos, G. V. Shlyapnikov, P. Zoller, and M. Lewenstein, *Phys. Rev. Lett.* **85**, 1791 (2000).
 - [39] M. Mayle, I. Lesanovsky, and P. Schmelcher, *Phys. Rev. A* **80**, 053410 (2009).
 - [40] G. Pupillo, A. Micheli, M. Boninsegni, I. Lesanovsky, and P. Zoller, *Phys. Rev. Lett.* **104**, 223002 (2010).
 - [41] T. Lahaye, C. Menotti, L. Santos, M. Lewenstein, and T. Pfau, *Rep. Prog. Phys* **72**, 126401 (2009).